DOI: 10.1002/ejic.201001133

In-situ Synchrotron X-ray Diffraction Study of the Formation of Cubic Li_2TiO_3 Under Hydrothermal Conditions

Andreas Laumann,[a] Kirsten Marie Ørnsbjerg Jensen,[b] Christoffer Tyrsted,[b] Martin Bremholm,[c] Karl Thomas Fehr,[a] Michael Holzapfel,[d] and Bo Brummerstedt Iversen*[b]

Keywords: Kinetics / Reaction mechanisms / Hydrothermal synthesis / Titanium / Lithium / Synchrotron diffraction

Synchrotron powder X-ray diffraction (PXRD) has been used to study in-situ the hydrothermal intercalation of lithium ions in titania powder following the reaction $TiO_2 + 2\ LiOH \rightarrow Li_2TiO_3 + H_2O$. Syntheses were performed in a sapphire capillary at temperatures between 133 and 230 °C. By sequential Rietveld refinement of the PXRD data, the particle growth of the metastable cubic α-Li_2TiO_3 compound was determined as a function of the reaction time, as well as the transformation of the cubic α-phase to its stable monoclinic β-modifications at a temperature above the critical point of water. The reactions were presumed to be controlled by nucleation and crystal growth, and therefore the Avrami-Erofe'ef equation was applied to model the reaction mechanisms of this intercalation process and an activation energy of 66(7) kJ/mol was determined.

Introduction

The compound Li_2TiO_3 exists in two structural modifications,[1] a cubic form of space group $Fm\bar{3}m$,[1–11] and a monoclinic structure of space group $C2/c$.[1,8–11] At low temperatures, the monoclinic form is stable, but it transforms to the cubic modification above ca. 1155 °C[1,8–12] before melting at ca. 1540 °C.[8–11] However, a metastable cubic modification can be produced at low temperatures by hydrothermal syntheses.[1–5] This metastable cubic modification is also known as α-Li_2TiO_3[1,10,11] and between 300 and 600 °C it transforms irreversibly to a monoclinic structure (β-Li_2TiO_3) e.g. in air[8–11] or in high vacuum.[1] Especially during the cubic-monoclinic transformation, β-Li_2TiO_3 is disordered due to stacking faults, which is indicated in the X-ray powder pattern by excessively sharp reflections of high intensity and missing, or very broad, reflections of low intensity, as well as by a reduced monoclinic β angle.[1] The final transformation to the well known ordered monoclinic β-Li_2TiO_3 of space group $C2/c$ occurs above 1000 °C.[1] The ordered structure is maintained upon cooling to room temperature.[1]

The crystal structure of the cubic Li_2TiO_3 phase is of the NaCl structure type, with a statistical distribution of lithium and titanium on one site, and oxygen on the other site.[1] The monoclinic structure in space group $C2/c$ can be derived from the parent cubic NaCl structure by the transformation

$$\begin{pmatrix} 1/2 & 1 & 1/2 \\ 3/2 & 0 & -3/2 \\ -3/2 & 1 & -3/2 \end{pmatrix}$$

from which the ideal monoclinic lattice constants $a_m = \sqrt{3/2}a_c$, $b_m = \sqrt{9/2}a_c$, $c_m = \sqrt{11/2}a_c$, and $\cos\beta_m = -1/\sqrt{33} \rightarrow \beta_m = 100.025°$ can be calculated. Ordering of the cations leads to a layered structure comprising three layers. The first layer only consists of lithium ions on 8*f* (Li1) and 4*d* (Li2) positions. The second layer is occupied by oxygen and the third layer has alternate titanium and lithium (Ti1, Ti2 and Li3) on 4*e* positions.

The compound α-Li_2TiO_3 can be produced by the hydrothermal reaction of anatase or rutile with lithium hydroxide for $LiOH/TiO_2 \geq 2$, and synthesis has been reported from a 2:1 ratio[1] up to a 50:1 ratio.[3] So far no other lithium titanium compounds than Li_2TiO_3 have been observed as products from the hydrothermal reaction of anatase or rutile in lithium hydroxide solution. Even when using a highly over-stoichiometric amount of lithium,[3] the surplus of lithium hydroxide remains unreacted and dissolved. Kinetic experiments of the hydrothermal formation of α-Li_2TiO_3 have

[a] Department of Earth and Environmental Sciences, Section for Mineralogy, Petrology und Geochemistry, Ludwig-Maximilians-Universität München,
Theresienstr. 41, 80333 Munich, Germany
[b] Centre for Materials Crystallography, Department of Chemistry and iNANO, Aarhus University,
Langelandsgade 140, 8000 Aarhus C, Denmark
Fax: +45-8619-6199
E-mail: bo@chem.au.dk
[c] Department of Chemistry, Princeton University,
Princeton, NJ 08544, USA
[d] Battery Materials, Süd-Chemie AG,
Ostenriederstr. 15, 85368 Moosburg, Germany
Supporting information for this article is available on the WWW under http://dx.doi.org/10.1002/ejic.201001133.

not been reported so far, whereas kinetic studies with divalent cations instead of lithium were performed in the system $ATiO_3$, where A = Ba, Ca, and Pb.[13–18]

Here, we report a time-resolved in-situ synchrotron powder X-ray diffraction (PXRD) study of the hydrothermal reaction of lithium hydroxide with titania. The kinetics of the formation of crystalline titania to α-Li_2TiO_3 were modelled for temperatures between 154 and 230 °C to determine the reaction mechanism.

Results

In all performed in-situ experiments, the hydrothermal reaction of titania in a lithium hydroxide solution to α-Li_2TiO_3 was recorded. The reaction can be expressed as

$$TiO_2(s) + 2\ LiOH(aq) \rightarrow Li_2TiO_3(s) + H_2O \quad (1)$$

At 133 °C, the lowest temperature of all performed experiments (EXP1), partial formation of Li_2TiO_3 was observed, but the kinetics were too slow for the complete formation of α-Li_2TiO_3 in a suitable time due to the restricted beam-time. The experiment was aborted after 26 min as the α-Li_2TiO_3 fraction was only ca. 20% and a high proportion of anatase and a minor proportion of rutile were still present. Higher temperatures lead to the complete formation of α-Li_2TiO_3 in less than 30 min (Table 1 and Figure 1).

Table 1. Temperature for each experiment, the times for the half-fraction, and the calculated values for the rate constant k (see kinetics section).

Run	T [°C]	$t_{1/2}$ [s]	k [s^{-1}][c]
EXP1[a]	133	–	–
EXP2	154	328.7	2.1×10^{-3}
EXP3[b]	168	156.1	4.4×10^{-3}
EXP4	169	121.5	5.7×10^{-3}
EXP5	195	38.9	1.8×10^{-2}
EXP6	215	22.7	3.1×10^{-2}
EXP7	230	21.1	3.3×10^{-2}

[a] Half-fraction was not reached within 30 min. [b] Experiment was heated to 420 °C after 22.5 min. holding time at 168 °C. [c] See kinetics section.

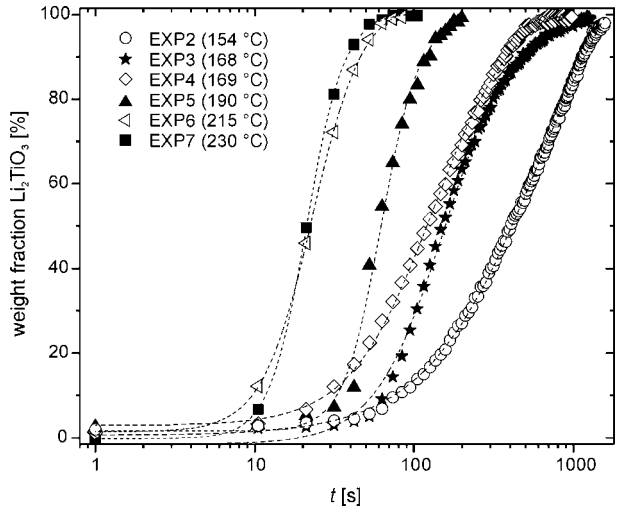

Figure 1. Data points and sigmoidal fits for the fractional progressions of EXP2–EXP7 vs. time.

The progress of all reactions could be fitted with a sigmoidal model. The fractional progress of α-Li_2TiO_3 and titania vs. time of EXP6 is plotted in detail in Figure 2, which shows an increasing fraction of the lithium titanate with a corresponding simultaneous decrease in the titania fraction. The temperature dependence of the half-fractions (α = 0.5) of Li_2TiO_3 displays an exponential decay, Figure 3.

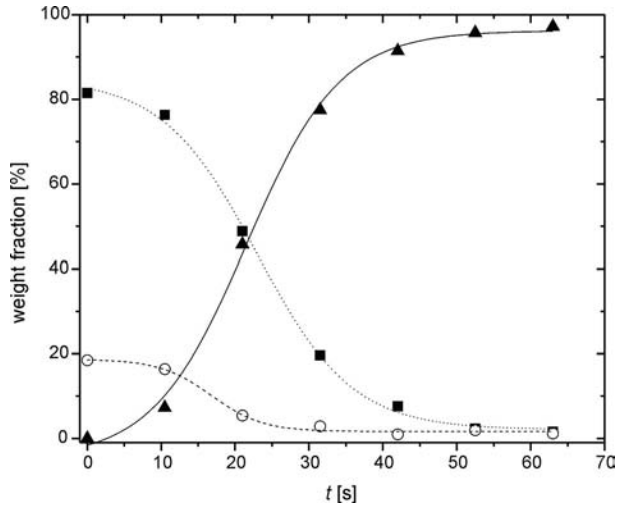

Figure 2. Fractional progression of anatase (squares) and rutile (circles) to α-Li_2TiO_3 (triangles) vs. time at 215 °C (EXP6) and sigmoidal fits of the formation of α-Li_2TiO_3 (solid) with the decay of anatase (dotted) and rutile (dashed).

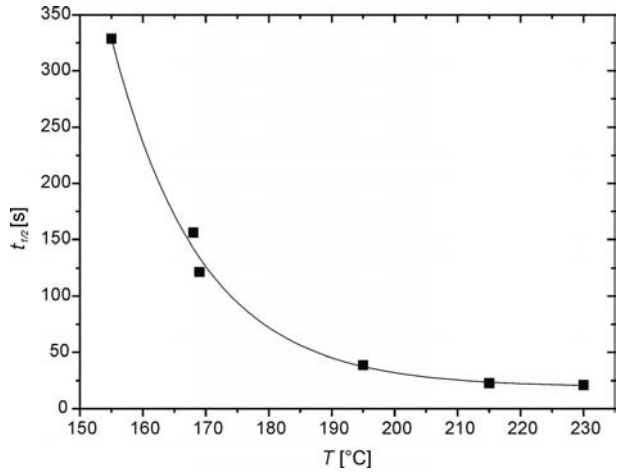

Figure 3. Half-fraction times, $t_{1/2}$, of the transformation to α-Li_2TiO_3 at different temperatures.

For EXP3, which was heated to 420 °C after 22.5 min, the progression of the reaction is shown in Figure 4. First, the formation of Li_2TiO_3 was observed with increasing intensity of the lithium titanate reflections and the diminishing reflections of titania, so that after about 18 min only reflections of lithium titanate were detected. The broad hump around 2Θ = 20° is caused by the aqueous lithium hydroxide solution in the sapphire capillary. Then, after 22.5 min, the temperature was set to 420 °C and the critical temperature of water (T_C = 374 °C) was crossed within a single detector exposure. The broad feature observed at a

temperature of 168 °C flattens as the fluid turns supercritical (Figure 4). At 420 °C, the reflections of the α-Li_2TiO_3 shift slightly to smaller 2Θ angles due to the thermal expansion of α-Li_2TiO_3. Moreover, new and broad reflections appear, whereof the reflection of the highest intensity at 2Θ ≈ 11.8° can clearly be ascribed to the (002) reflection of the monoclinic β-Li_2TiO_3 phase. Especially in the beginning of the cubic to monoclinic transformation, the monoclinic Li_2TiO_3 is disordered due to stacking faults[1] and it was not possible to refine the FWHM parameters (see discussion).

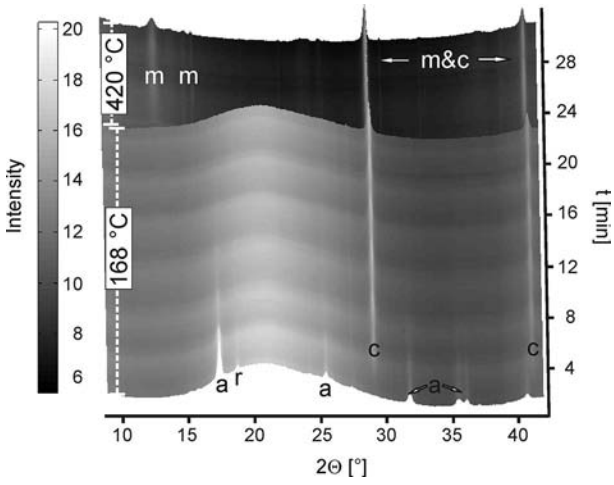

Figure 4. Three dimensional plot of diffraction data showing the transformation from anatase (a) and rutile (r) to the cubic α-Li_2TiO_3 (c) at 168 °C (EXP3). Heating to 420 °C after 23 min results in the beginning of the transformation from α-Li_2TiO_3 to the monoclinic β-Li_2TiO_3 (m). The broad hump around 2θ = 20° is caused by the lithium hydroxide solution.

Modelling of Anatase and α-Li_2TiO_3 Particles

The refined nanocrystal size of P25 yielded a value of ca. 20 nm, which is in good agreement with the specification of Evonik (21 nm). P25 comprises anatase and rutile in a ratio of 4:1, thus a reasonable refinement of the particle size of rutile was only possible at the very beginning of each experiment. Therefore, sequential refinement of the size of the anatase particles produced better results, especially for reactions at lower temperatures, where anatase was detectable over a longer period.

Anatase can be described in the tetragonal space group $I4_1/amd$ with unit cell parameters a = 3.785(1) Å and c = 9.482(3) Å.[19] The structure has various empty octahedral sites, where lithium possibly can be accommodated.[20–23] The unit cell parameters of anatase at the onset of all experiments show some minor variations compared with the theoretical values. These small changes are probably caused by a small displacement of the capillary due to the heating. With ongoing reaction time, the unit cell parameters changed and the values of the unit cell parameter a increased slightly and the values of the unit cell parameter c decreased, stronger with longer reaction time and particularly before the full cell formation of α-Li_2TiO_3 was accomplished (Figure 5). The particle size of anatase remained fairly constant until the lithium intercalation was completed (Figure 6).

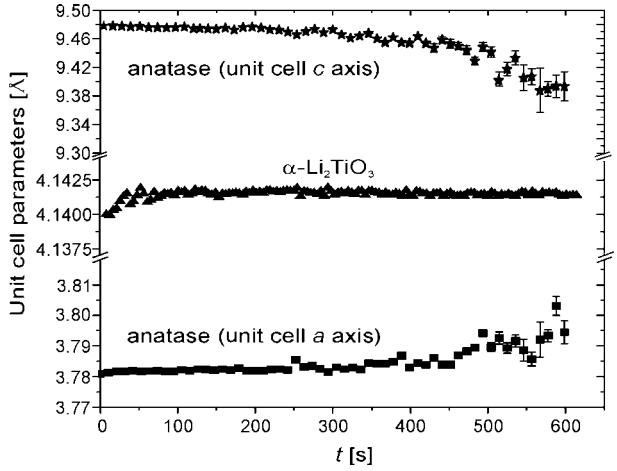

Figure 5. Progression of unit cell a axis (squares) and unit cell c axis (stars) of anatase and the constant unit cell of α-Li_2TiO_3 (triangles) with time and ongoing formation of α-Li_2TiO_3 (EXP2, 154 °C).

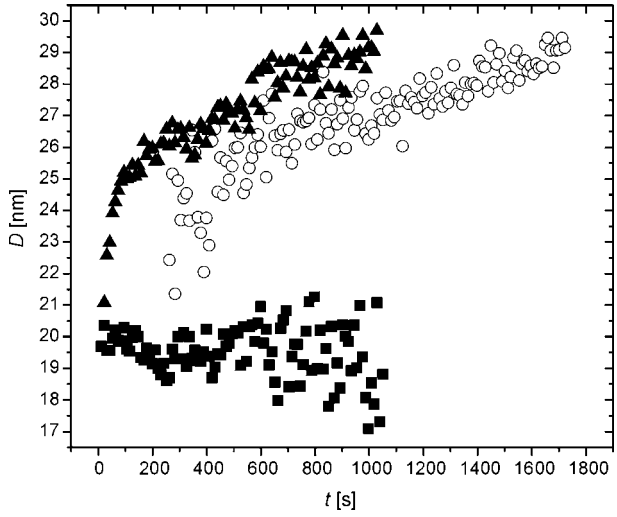

Figure 6. Particle growth of α-Li_2TiO_3 in EXP2 (circles) and in EXP6 (triangles), and the size of the anatase particles in EXP2 (squares) vs. reaction time (error approx. 1 nm). Due to the low fraction of α-Li_2TiO_3 in EXP2 before 250 s the FWHM parameters could not be refined. The same problem occurred for anatase particles after 1000 s. Both are indicated by the wider scattering of the data points of α-Li_2TiO_3 at the beginning of the formation and for anatase, when only a low fraction is left.

The unit cell parameter of the α-Li_2TiO_3 particles seem to increase slightly at the very beginning of each experiment, which also could be caused by errors in the refinement due to low fraction of the titanate. Then, during the formation to α-Li_2TiO_3 and until the experiments were aborted, the unit cell parameter stayed constant around 4.14 Å (Figure 5). The first detectable α-Li_2TiO_3 particles showed approximately the same size as the crystalline tita-

nia reactant P25 (Figure 6). With ongoing reaction time, the lithium titanate particles grew, slightly faster at higher temperatures. The two experiments with the highest synthesis temperature showed a similar fast particle growth, and in EXP6 the particle growth is ca. 8 nm within 1000 s (Figure 6).

Kinetics

As mentioned before, the increase of the fractions of the lithium titanate, as well as the decrease of the fractions of the titania powders, show a sigmoidal reaction progress, suggesting that nucleation and crystal growth control the reaction.[15] In solid state chemistry, the Avrami-Erofe'ef equation[24–27] is broadly applied to model phase transformations, nucleation and crystal growth. It relates the fraction of a reaction, α, at each temperature by using the relationship

$$\alpha = 1 - \exp[-k(t - t_0)^n] \quad (2)$$

where n is the Avrami exponent, t_0 the induction time, and k the rate constant. The exponent n gives details about the rate of nucleation and the mechanism of nuclei growth. The expression is most valid in the fractional range from $0.15 < \alpha < 0.5$. Reactions of the present study were fast, so that for EXP5, EXP6 and EXP7 only one or two data points would be found in the $0.15 < \alpha < 0.5$ range, and therefore these experiments are not included in the following considerations. The value of n can be determined by applying a Sharp–Hancock plot,[28] which is a plot of $\ln[-\ln(1 - \alpha)]$ vs. $\ln(t)$. This gives a straight line with a slope of n. Changes in the reaction mechanism can be identified as a change in the slope. At low fractions, the experiments EXP2, EXP3 and EXP4 show a slope of ca. 2. The reaction mechanism seems to change at about $\alpha = 0.35$, as is especially evident for EXP2. Thus, the range of $0.15 < \alpha < 0.85$ was applied for EXP2, EXP3 and EXP4 (Figure 7). At fractions $\alpha \approx 0.45$, the slope is less steep in all of the three experiments and an average value of $n \approx 1.2$ is obtained.

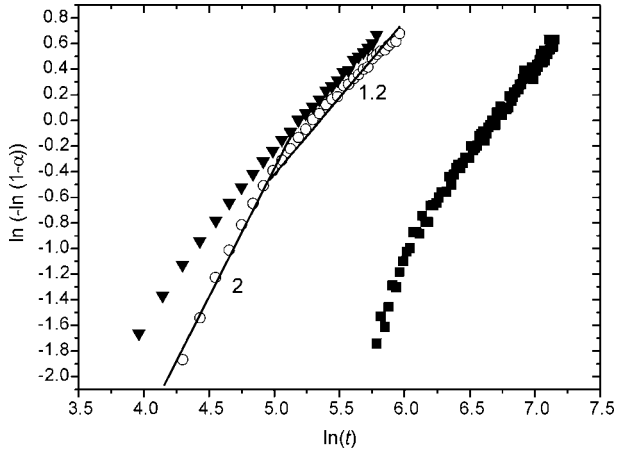

Figure 7. Sharp–Hancock plot for the transformation of P25 titania powder in lithium hydroxide solution to α-Li_2TiO_3 at 154 °C (squares), 168 °C (circles) and 169 °C (triangles).

In order to calculate the activation energy for the crystallization of α-Li_2TiO_3, $\ln(k)$ against $1/T(\mathrm{K}) \times 1000$ is plotted, displaying the logarithmic form of the Arrhenius equation

$$k = A \cdot \exp(-E_A/RT) \quad (3)$$

where A is the pre-exponential factor, E_A the effective activation energy, R the gas constant, and T the absolute temperature. The calculated values are listed in Table 1 and the Arrhenius plot in Figure 8 displays $\ln(k)$ vs. $1/T \times 1000$. E_A can be calculated from the slope of the plot, which gives a value of 66(7) kJ/mol.

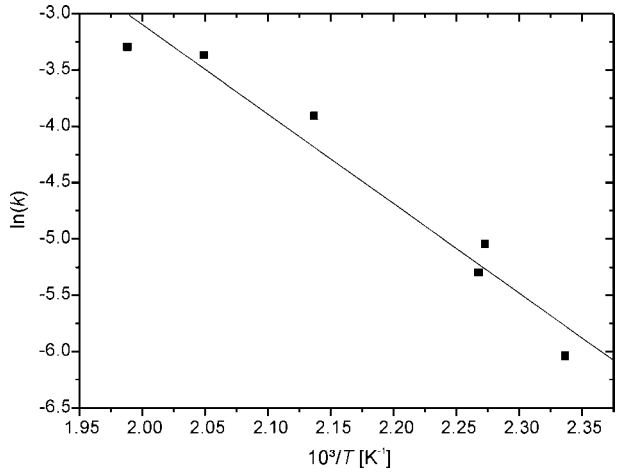

Figure 8. Arrhenius plot used to determine the activation energy of the intercalation of lithium in titania.

Discussion

Lithium Intercalation in Titania Powder

The unit cell parameters of anatase change during the formation of α-Li_2TiO_3, as shown in Figure 5. This observation might be explained by lithium ions inserting the anatase structure, without yet transforming to α-Li_2TiO_3. The simultaneous decrease of the titania fraction and the growth of the lithium titanate (Figure 2) proves that lithium intercalates the titania particles, i.e. a direct reaction to α-Li_2TiO_3 takes place without a prior formation of e.g. a $Ti(OH)_4$ phase, which has been proposed for the hydrothermal synthesis of $BaTiO_3$.[15] The comparable particle sizes of reactant and the first formed products (Figure 6) also suggests that lithium ions are intercalated in the titania structure without dissolving of the titania particles. Hypothesizing that the reaction mechanism is controlled by dissolution and recrystallization, one would expect a decrease in the average particle size of the titanium oxide precursors prior to and during the crystallization of the Li_2TiO_3. The constant size of the anatase indicates that a dissolution-recrystallization mechanism can be excluded and suggests a topotactic transformation mechanism.

Most studies on the intercalation of lithium ions in titania were performed by electrochemical intercalation of lithium e.g. in anatase.[20–23] By electrochemical intercalation,

Ti^{4+} is partially reduced to Ti^{3+}, and compositions of $Li_x(Ti^{3+}{}_xTi^{4+}{}_{1-x})O_2$ are obtained. For $x < 0.25$ the tetragonal anatase structure is maintained. The unit cell parameter a increases with lithium insertion, while c decreases,[21,22] as also observed in the present study (Figure 5). However, the reaction taking place here is hardly comparable with the electrochemical intercalation of lithium in anatase, as titanium is unlikely to be reduced under the present conditions. Nevertheless, before the anatase phase finally transforms to α-Li_2TiO_3, lithium ions might fill empty sites of the anatase structure and cause the minor change of the unit cell parameters. This will occur at the end of each reaction, when most of the anatase is already transformed to α-Li_2TiO_3 and in the remaining anatase some lithium ions will already have intercalated.

Cubic-Monoclinic Transformation of Li_2TiO_3

The transformation of the metastable α-Li_2TiO_3 to the monoclinic Li_2TiO_3 above 300 °C was so far only described in air or vacuum[1,5,8–11] and it takes place over a wide temperature range. The complete transformation to the β-phase occurs above 500 °C[1] and at 420 °C a two-phase system comprising the cubic and the monoclinic structure is expected. Lithium has a low X-ray scattering power and all reflections of the cubic phase are superimposed on the reflections of the monoclinic phase. Thus, the FWHM parameters had to be fixed, and the refined fraction of 47(1)% of the cubic phase at 420 °C must be considered as a first estimate only, which however compares well with fractions of the cubic phase [60(2)%] at 400 °C and at 500 °C [11.5(7)%] reported by Laumann et al.[1] This leads to the assumption, that the cubic to monoclinic transformation occurs at a similar temperature, irrespective of whether a dry powder is heated in high vacuum or in aqueous lithium hydroxide solution above the critical point of water.

Reaction Mechanism

The slope n which is obtained from Equation (3) can give information about the mechanisms of the reactions. According to Sharp and Hancock,[28] for n = 0.54–0.62 a diffusion-limited rate is inferred, where the rate of diffusion of the reactive species to the nucleation sites is the rate-determining step. For n = 1.0–1.24, a zero-order, first-order, or a phase boundary mechanism between the product and the reagent mixture is rate determining, and for n = 2.0–3.0, the formation of nucleation sites is the process that controls the rate. In the present study, the slope n = 2 in the beginning of the reactions (Figure 7) suggests that the nucleation of Li_2TiO_3 sites is the rate-determining step. As no sign of dissolution of the titania particles was observed, the formation of Li_2TiO_3 does not occur from solution, but rather formation of Li_2TiO_3 domains occur from within the titania particles. Then, the slope becomes less steep at higher fractions and $n \approx 1.2$ suggests that once enough Li_2TiO_3 nuclei are formed, the reaction mechanism changes, and then the reaction at the phase boundary is the rate determining mechanism at higher fractions. The rather high activation energy of 66(7) kJ/mol also suggests a phase boundary or nucleation controlled mechanism. $E_A < 32$ kJ/mol would be an indicator for diffusion controlled process.[29]

The present study focused on the reaction of the titania powder P25 with a 0.5 M lithium hydroxide solution. It is expected, that by using other titania reactants, or a higher or less concentrated lithium hydroxide solution, the kinetics, and even the reaction mechanisms might change. For the formation e.g. of $BaTiO_3$, the activation energies were found to depend mainly on the titania reactant,[16] thus for $BaTiO_3$ various activation energies between 21 kJ/mol[30] and 105.5 kJ/mol have been reported.[31] For the hydrothermal formation of the lithium titanate it was reported that coarser particles (ca. 100 nm) cause problems to fulfil a complete reaction at 160 °C,[5] whereas by using a 5 nm anatase, lithium intercalation can be performed in a 2.5 M lithium hydroxide solution at 60 °C.[32] Obviously, a faster reaction at the same temperature can be expected for a higher concentration of the lithium hydroxide solution. Here, especially at low temperatures, e.g. in EXP2 (154 °C) the reaction is slowed down before getting to the end of the complete formation of α-Li_2TiO_3, indicating that low concentrations of remaining lithium ions in the solution decelerate the kinetics (see Figure 1).

Conclusions

For the first time, in-situ synchrotron radiation has been used to study the interaction of titania powder in a lithium hydroxide solution under hydrothermal conditions. Lithium ions were found to intercalate in the titania structure without a prior dissolution of the titania compounds and the particle growth of the formed metastable cubic α-Li_2TiO_3 was recorded. Upon heating the suspension of α-Li_2TiO_3 particles in a lithium hydroxide solution above the critical point of water, α-Li_2TiO_3 was found to transform to the monoclinic β-Li_2TiO_3 in a similar way as observed for dry α-Li_2TiO_3 powder heated in air or in high vacuum. By applying the Avrami-Erofe'ef equation, the rate controlling mechanism could be determined for the reactions at lower temperatures. The process was found to be non-isokinetic due to a change from a nucleation controlled to a phase boundary controlled reaction, which may depend on the used titania reactant and the concentration of the lithium hydroxide solution. The calculated activation energy of 66(7) kJ/mol also will be sensitive to variations of the reaction conditions.

Experimental Section

Synthesis: All experiments were performed using an aqueous suspension of titania powder (Evonik, formerly Degussa, AEROXIDE TiO_2 P25) and dissolved lithium hydroxide (SQM, Chile). P25 comprises anatase and rutile in a ratio of about 4:1. Before the synchrotron experiments were started, 0.4 g of P25 and 0.58 g of $LiOH{\cdot}H_2O$ were stirred in 25 mL of de-ionized water for 1 h in air. In total, kinetic data of 7 experiments, denoted EXP1 to EXP7

with increasing number for higher syntheses temperatures, were conducted. The adjusted temperatures were 133, 154, 168, 169, 195, 215 and 230 °C at a pressure of 230 bar. In addition EXP3 was subsequently heated to the maximal possible temperature of 420 °C after a holding time of 22.5 min at 168 °C.

Setup: The in-situ synchrotron data was recorded at beamline I711 at MAX-lab in Lund, Sweden.[33] The syntheses were performed in a custom build reactor[34–36] using a sapphire capillary with an inner diameter of 0.7 mm. For all experiments, the suspension was injected into the capillary with a syringe. The capillary was aligned in the X-ray beam, pressurized to 230 bar, and then heated to the desired temperature in a hot air flow. The temperature in the capillary was measured with a thermocouple right next to the beam. The reactor design has been described in detail elsewhere.[34,36]

Data Analysis: The wavelength was adjusted to 0.997 Å and the detector had a time resolution of 10.5 s per frame. The 2D diffraction data were integrated in the program Fit2D,[37] and subsequently, the time resolved PXRD data sets were analyzed by sequential Rietveld refinement using the program FullProf.[38] The peaks were fitted with the Thompson–Cox–Hastings pseudo-Voigt axial divergence asymmetry peak shape,[39] and the Gaussian and Lorentzian full width at half maximum (FWHM) is calculated from

$$FWHM_G^2 = (U + e^2)\tan^2\Theta + V\tan\Theta + W \quad (3)$$

$$FWHM_L^2 = (Y + \lambda/L)/\cos\Theta \quad (4)$$

where U, V, W and Y are the instrumental resolution parameters (obtained from a LaB_6 standard sample), λ is the wavelength, and $e = \Delta d/d$ and L are the "apparent" strain and size parameters, respectively. The atomic coordinates of anatase,[19] rutile,[40] the cubic Li_2TiO_3[1] and the monoclinic Li_2TiO_3[1] were fixed at the values from the literature. The isotropic thermal parameters (B_{iso}) were fixed to 1, a reasonable value higher than the room temperature data of Kataoka et al.[12] Test refinements with both lower and higher B_{iso} values showed negligible influence on the particle size and no influence on the observed trends.

The background was linearly interpolated between a set of background points with refinable intensity. In the Supporting Information specific examples of Rietveld refinements are shown together with relevant crystallographic details.

Supporting Information (see footnote on the first page of this article): Two dimensional PXRD data for all experiments and selected examples of Rietveld refinements of data sets from EXP6 and EXP3 with corresponding crystallographic information.

Acknowledgments

We would like to thank Mogens Christensen, Nina Lock, Jacob Becker-Christensen and Yngve Cerenius for help during measurements at the MAX-II synchrotron in Lund. Funding of this project was provided by the Danish Strategic Research Council (CEM), The Danish National Research Foundation (CMC), the Danish Research Council for Nature and Universe (Danscatt) and Süd-Chemie AG, Germany.

[1] A. Laumann, K. T. Fehr, H. Boysen, M. Hoelzel, M. Holzapfel, *Z. Kristallogr.* **2011**, *226*, 53.
[2] H. Song, H. Jiang, T. Liu, X. Liu, G. Meng, *Mater. Res. Bull.* **2007**, *42*, 334.
[3] M. Tomiha, N. Masaki, S. Uchida, T. Sato, *J. Mater. Sci.* **2002**, *37*, 2341.
[4] M. Tabuchi, A. Nakashima, H. Shigemura, K. Ado, H. Kobayashi, H. Sakaebe, K. Tasumi, *J. Mater. Chem.* **2003**, *13*, 1747.
[5] A. Laumann, K. T. Fehr, M. Holzapfel, M. Wachsmann, B. B. Iversen, *Solid State Ionics* **2010**, *181*, 1525.
[6] E. Kordes, *Fortschr. Mineral. Kristallogr. Petrogr.* **1933**, *17–18*, 27.
[7] E. Kordes, *Z. Kristallogr.* **1935**, *92*, 139.
[8] C. Gicquel, M. M. Mayer, R. Bouaziz, *C. R. Acad. Sci. Paris Série C* **1972**, *275*, 1427.
[9] J. C. Mikkelsen, *J. Am. Ceram. Soc.* **1980**, *63*, 331.
[10] H. Kleykamp, *J. Nucl. Mater.* **2001**, *295*, 244.
[11] H. Kleykamp, *Fusion Eng. Des.* **2002**, *61–62*, 361.
[12] K. Kataoka, Y. Takahashi, N. Kijima, H. Nagai, J. Akimoto, Y. Idemoto, K. Ohshima, *Mater. Res. Bull.* **2009**, *44*, 168.
[13] J. O. Eckert Jr., C. C. Hung-Houtson, B. L. Gersten, M. M. Lencka, R. E. Riman, *J. Am. Ceram. Soc.* **1996**, *79*, 2929.
[14] J. Moon, E. Suvaci, A. Morrone, S. A. Costantino, J. H. Adair, *J. Eur. Ceram. Soc.* **2003**, *23*, 2153.
[15] A. Testino, V. Buscaglia, M. T. Buscaglia, M. Viviani, P. Nanni, *Chem. Mater.* **2005**, *17*, 5346.
[16] R. I. Walton, F. Millange, R. I. Smith, T. C. Hansen, D. O'Hare, *J. Am. Chem. Soc.* **2001**, *123*, 12547.
[17] D. Croker, M. Loan, B. K. Hodnett, *Cryst. Growth Des.* **2009**, *9*, 2207.
[18] G. A. Rosetti Jr., D. J. Watson, R. E. Newnham, J. H. Adair, *J. Cryst. Growth* **1992**, *116*, 251.
[19] I. Djerdj, A. M. Tonejc, *J. Alloys Compd.* **2006**, *413*, 159.
[20] M. V. Koudriachova, S. W. de Leeuw, *Phys. Rev. B* **2004**, *69*, 0541016–1.
[21] F. Tielens, M. Calatyud, A. Beltrán, C. Minot, J. Andrés, *J. Electroanal. Chem.* **2005**, *581*, 216.
[22] M. Wagemaker, G. J. Kearley, A. A. van Well, H. Mutka, F. M. Mulder, *J. Am. Chem. Soc.* **2003**, *125*, 840.
[23] M. Wagemaker, A. A. van Well, G. J. Kearley, F. M. Mulder, *Solid State Ionics* **2004**, *175*, 191.
[24] M. J. Avrami, *J. Chem. Phys.* **1939**, *7*, 1103.
[25] M. J. Avrami, *J. Chem. Phys.* **1940**, *8*, 212.
[26] M. J. Avrami, *J. Chem. Phys.* **1941**, *9*, 177.
[27] B. V. C. Erofe'ev, *R. Dokl. Acad. Sci. SSSR* **1946**, *52*, 511.
[28] J. D. Hancock, J. H. Sharp, *J. Am. Ceram. Soc.* **1972**, *55*, 74.
[29] A. C. Lasagna, *Kinetic Theory in the Earth Sciences*, Princeton University Press, **1998**.
[30] N. A. Ovramenko, L. I. Shevts, F. D. Ovcharenko, B. Y. Komilovich, *Izv. Akad. Nauk SSSR, Neorg. Mater.* **1979**, *248*, 889.
[31] W. J. Hertl, *J. Am. Ceram. Soc.* **1988**, *71*, 879.
[32] C. Jiang, E. Hosono, M. Ichihara, I. Honma, H. Zhou, *J. Electrochem. Soc.* **2008**, *155*, A553.
[33] Y. Cerenius, K. Ståhl, L. A. Svensson, T. Ursby, Å. Oskarsson, J. Albertsson, A. Liljas, *J. Synchrotron Radiat.* **2000**, *7*, 203.
[34] M. Bremholm, H. Jensen, S. B. Iversen, B. B. Iversen, *J. Supercrit. Fluids* **2008**, *22*, 385.
[35] C. Tyrsted, J. Becker, P. Hald, M. Bremholm, J. S. Pedersen, J. Chevallier, Y. Cerenius, S. B. Iversen, B. B. Iversen, *Chem. Mater.* **2010**, *22*, 1814.
[36] J. Becker, M. Bremholm, C. Tyrsted, B. Pauw, K. M. Ørnsbjerg Jensen, J. Eltzholt, M. Christensen, B. B. Iversen, *J. Appl. Crystallogr.* **2010**, *43*, 729.
[37] A. P. Hammersley, S. O. Svensson, M. Hanfland, A. N. Fitch, D. Häusermann, *Adv. High Pressure Res.* **1996**, *14*, 235.
[38] J. Rodriguez-Carvajal, *Physica B* **1993**, *192*, 55.
[39] P. Thompson, D. E. Cox, J. B. Hastings, *J. Appl. Crystallogr.* **1987**, *20*, 79.
[40] X. Bokhimi, A. Morales, F. Pedraza, *J. Solid State Chem.* **2002**, *169*, 176.

Received: October 23, 2010
Published Online: March 30, 2011

